Distribution Agreement

In presenting this thesis as a partial fulfillment of the requirements for a degree from Emory University, I hereby grant to Emory University and its agents the non-exclusive license to archive, make accessible, and display my thesis in whole or in part in all forms of media, now or hereafter now, including display on the World Wide Web. I understand that I may select some access restrictions as part of the online submission of this thesis. I retain all ownership rights to the copyright of the thesis. I also retain the right to use in future works (such as articles or books) all or part of this thesis.

Christian David Gonzalez April 7th 2014

Investigating the expression profile of the *Scn8a* voltage-gated sodium channel in the cerebral cortex and the thalamus

by

Christian David Gonzalez

Andrew Escayg
Adviser

Emory College Department of Neuroscience and Behavioral Biology

Andrew Escayg

Adviser

Leah Roesch

Committee Member

Yoland Smith

Committee Member

2014

Investigating the expression profile of the *Scn8a* voltage-gated sodium channel in the cerebral cortex and the thalamus

by

Christian D Gonzalez

Andrew Escayg

Adviser

An abstract of
a thesis submitted to the Faculty of Emory College of Arts and Sciences
of Emory University in partial fulfillment
of the requirements of the degree of
Bachelor of Sciences with Honors

Emory College Department of Neuroscience and Behavioral Biology

2014

Abstract

Investigating the expression profile of the *Scn8a* voltage-gated sodium channel in the cerebral cortex and thalamus

By Christian D Gonzalez

Neuronal communication is dependent on the generation of action potentials. The normal functioning of voltage-gated sodium channels is required for the generation of an action potential. *Scn8a* mutations in mice, mutations in a channel coding for voltage-gated sodium channel six ($Na_v1.6$), are associated with the generation of spike-wave discharges (SWDs) and absence epilepsy (Papale et al., 2009). Absence epilepsy is a non-convulsive form of genetic generalized epilepsy showing characteristic SWDs on EEG recordings of patients afflicted with this condition. Several studies have established that SWDs arise from disturbances in the thalamocortical circuitry (Lacey et al., 2012 ; Seidenbecher et al., 1998). Although it is known that certain genetic factors may contribute to absence epilepsy, a full understanding of the genetic, molecular and cellular mechanisms of absence epilepsy remains elusive. The purpose of this study was to survey the expression of *Scn8a* in the cerebral cortex, reticular nucleus, hippocampus, and thalamus of the mouse in order to further elucidate the mechanisms which underlie absence seizure generation. Using immunohistochemistry and fluorescence imaging, we observed broad *Scn8a* expression and confirmed that *Scn8a* is expressed in GABAergic neurons in various regions of the mouse brain. We found that the expression of *Scn8a* varies between different brain structures and layers of the cortex. Based on these results, we developed a model which may explain how SWDs arise from altered *Scn8a* function.

Investigating the expression profile of the *Scn8a* voltage-gated sodium channel in the cerebral cortex and the thalamus

By

Christian D Gonzalez

Andrew Escayg

Adviser

A thesis submitted to the Faculty of Emory College of Arts and Sciences
of Emory University in partial fulfillment
of the requirements of the degree of
Bachelor of Sciences with Honors

Emory College Department of Neuroscience and Behavioral Biology

2014

Acknowledgements

I would like to extend my gratitude to my graduate mentor Dr. Christopher D Makinson for introducing me and guiding me through my research experience at the Escayg laboratory.

I would like to thank the principal investigator of my lab and my adviser Andrew Escayg for aiding me through this Honors Thesis project and for allowing me to work in his laboratory. It was a pleasure and a great college experience.

I would also like to thank Dr. Leah Roesch for being part of my committee and providing me with sound advice during my years at Emory.

I would like to thank Dr. Yoland Smith for being part of my committee and for being so willing to help me during my Honors Project.

Table of Contents

Contents

Introduction

Epilepsy is a neurological condition characterized by recurrent seizures. Seizures are defined by abnormal synchronous high amplitude electrical activity in the brain that is usually associated with neuronal hyper-excitability. Epilepsy affects about 2 million people in the United States and accounts for $15.5 billion in direct and indirect costs each year. One-third of the people affected by epilepsy are refractory to available antiepileptic drugs (AEDs) indicating the need for the development of more efficacious treatments (NCCDPHP, 2011).

Neuronal communication relies on the use of the action potential, a self-propagating mechanism dependent on the movement of ions across the neuronal membrane. It thus follows that the proteins which allow for the movement of these ions across the neuronal membrane are essential for neuronal communication. Of particular interest are the protein channels that respond to changes in the membrane potential difference of the neuron, these are known as voltage-gated channels. Various types of voltage-gated ion channels exist that respond to various voltages and are permeable to different types of ions. The initiation and propagation of action potentials in mammalian neurons is heavily dependent on the normal functioning of voltage-gated sodium channels (Meisler et al., 2005). Voltage-gated sodium channels consist of four homologous transmembrane domains, each consisting of six segments (S1-S6). The S5-S6 linker of each domain assembles to form a pore through the neuronal membrane that is permeable to sodium ions. In addition to the pore forming alpha subunits, there are also beta subunits, coded by another set of genes, which influence the kinetics, level of expression and voltage sensitivity of the voltage-gated sodium channel (Isom et al., 1994; Meisler et al., 2005; Yu et al., 2003). There are four highly expressed voltage-gated sodium channel alpha subunits in the mammalian central

nervous system. These are coded by the following genes: *SCN1A*, *SCN2A*, *SCN3A* and *SCN8A*. These genes express $Na_v1.1$, $Na_v1.2$, $Na_v1.3$ and $Na_v1.6$, respectively. The high degree of evolutionary conservation of these genes allows for the use of model systems during experimentation.

Mutations in these genes as well as the genes coding the beta subunits have been observed in various human epileptic phenotypes. Beta subunit mutations most likely affect the function of the voltage-gated sodium channel's inactivation gate resulting in neuronal hyperexcitability (Meisler et al., 2005). More than 700 mutations of the *SCN1A* gene have been identified in patients with Dravet syndrome, making this the most commonly mutated gene in human epilepsy (Meisler et al., 2010). Mutations in *SCN2A*, *SCN3A* and *SCN8A* have also been found.

In addition to epilepsy, *SCN8A* mutations are also associated with ataxia, behavioral abnormalities and mental deficits in humans and movement disorders in mice (Buchner et al., 2004; Hawkins et al, 2011). In mice, tremor and loss of hind limb function are observed in homozygous *Scn8a* mutants, and null homozygous mutants do not survive beyond 3-4 weeks of age (Levin et al., 2006). Electrophysiological recordings of neurons from mice with *Scn8a* mutations have revealed that the sodium current generated by the neurons is affected and the specific functional effect of the mutation is dependent on the type of neurons (Maurice et al., 2001). Electrophysiological analyses have also shown that this channel is responsible for the resurgent flow that occurs during repolarization, and contributes to persistent and subthreshold sodium current in various types of neurons (Cummins et al., 2005; Maurice et al., 2001; Van Wart et al., 2006). *SCN8A* mutations, and the resulting $Na_v1.6$ dysfunction result in a reduction in the persistent subthreshold sodium current (Do et al., 2004). Within the last few years,

exploration of a few of these *SCN8A* mutations has shed light on the role of *SCN8A* in seizure generation. We recently found that *Scn8a*$^{med\text{-}jo/+}$ mutants that carry a missense mutation in *Scn8a* and *Scn8a*$^{med/+}$ mutants with a loss-of-function *Scn8a* mutation are more resistant to flurothyl- and kainic acid-induced seizures (Martin et al., 2007). We then crossed the *Scn8a*$^{med\text{-}jo/+}$ mutants with a heterozygous *Scn1a* knockout mouse (*Scn1a*$^{+/-}$) — the *Scn1a*$^{+/-}$ mutants have lower seizure thresholds than wild type control mice (Martin et al., 2007)— and observed that the seizure threshold was restored to normal levels in progeny that expressed mutations in both genes. The premature lethality of the *Scn1a*$^{+/-}$ mice was also decreased in the presence of the *Scn8a* mutation (Martin et al., 2007). We then studied electroencephalographic recordings (EEG) and behavioral characteristics of three mutant *Scn8a* alleles. It was concluded that these heterozygous mutants showed EEG and behavioral characteristics similar to that of absence seizures in humans (Papale et al., 2009). Furthermore, the frequency of spike-wave discharge was decreased in response to ethosuximide, a drug used to treat absence epilepsy in humans (Papale et al., 2009).

Absence epilepsy is a non-convulsive form of idiopathic generalized epilepsy that is characterized by recurrent seizures in patients without brain lesions. It often occurs in childhood and adolescence, with a prevalence of ~10% among children with any type of epilepsy. Typical absence seizures are associated with spike-wave discharges of 3-4 Hz in frequency on electroencephalographic recordings, as well as brief loss of awareness that follows the onset of the spike-wave discharges (Papale et al., 2009). Although it is known that certain genetic factors may contribute to absence epilepsy, a full understanding of the genetic, molecular and cellular mechanisms of absence epilepsy remain elusive. However, there are studies that show the spike-wave discharge characteristic of absence seizure is a result of disturbances in thalamocortical

circuitry (Lacey et al., 2012 ; Seidenbecher et al., 1998). The thalamocortical circuit consists of neuronal interactions between the cortex, the thalamus and the reticular nucleus of the thalamus.

Studies on absence epilepsy have found that spike-wave discharges (SWDs) result from an abnormal oscillatory pattern of discharge involving mutually interconnected cortical and thalamic neurons (Seidenbecher et al., 1998). Moreover, these SWDs are generated by the same circuitry that sustains the spindle waves that appear on EEG recordings during the early stages of slow wave sleep (Steriade et. Al, 1993).The thalamocortical circuitry that results in these spindle oscillations has been shown to be initiated by spontaneously generated action potentials in the reticular nucleus of the thalamus. These GABAergic neurons synapse onto thalmocortical neurons which project their axons to the cortex and have collaterals which return to the reticular nucleus of the thalamus (McCormick & Bal, 1997). The generation of SWDs has been associated with concurrent rhythmic burst activity in the reticular nucleus of the thalamus, somatosensory thalamic nuclei and the cortex. They have also been associated with burst like firing at a temporal sequence that occurs in the cortex prior to the SWD (Seidenbecher et al., 1998).

Other studies have classified excitation of the reticular nucleus of the thalamus as being responsible for maintaining intrathalamic or enhancing thalamocortical seizure-related activity (Lacey et al., 2012). In exploring differential genetic expression of the cortex in an absence epilepsy model, using a WAG/Rij mouse line, Klein et al. (2003) found that *Scn1a* and *Scn8a* are up-regulated in cortical layers 1-4. More recently, our lab found that selectively reducing the expression of *Scn8a* in inhibitory neurons results in SWDs, whilst reducing Scn8a expression in excitatory cell types does not generate the characteristic absence epilepsy behavior (Makinson 2014).

The purpose of this study was to survey the expression of *SCN8A*, a gene involved in absence epilepsy, in various regions of the brain involved in absence seizure generation, such as the cortex, the reticular nucleus, the hippocampus and the thalamus to further elucidate the mechanisms which underlie absence seizure generation.

Materials and Methods

Animals

C3HeB/FeJ-*SCN8A*^{med}/J, B6;129S6-Gt(ROSA)26Sortm9(CAG-tdTomato)Hze/J and C57BL/6J mice were purchased from the Jackson Laboratory, Bar Harbor and the med male mutants were maintained on C3HeB/FeJ background. All mice were housed in a pathogen-free mouse facility with a 12-hour light/dark cycle. Food and water were freely available to the mice (*ad libitum*). The institutional Animal Care and Use Committee (IACUC) at Jackson Laboratory and Emory University approved all experimental protocols involving these mice.

Perfusion of Animals

Animals were deeply anesthetized by using 0.2 mL of isoflurane administered in a small chamber. Once anesthetized, cardiovascular perfusion was initiated by injection of 30 mL 1X PBS solution (10X PBS: 80 g NaCl, 2 g KCl, 14.4 g Na_2HPO_4 dibasic anhydrous and 2.4 g KH_2PO_4 monobasic anhydrous all in a 1 L aqueous solution adjusted to 7.3 pH with H_3PO_4). Then, either 30 mL of 4% paraformaldehyde (4%PFA: 40 g paraformaldehyde, 6 drops 10 N NaOH and 100 mL 10X PBS all in 1 L aqueous solution adjusted to 7.3 pH with HCl) or 1% paraformaldehyde (a dilution of the 4 % PFA solution) were perfused through the cardiovascular

system of the animal. Brains were then excised and submerged in the same concentration fixative used for the perfusion for 2 hours. After the 2 hours, the brain was placed in 20 mL of 30% sucrose aqueous solution and left at 4°C until the brain sank to the bottom of the container. After the brain was fully submerged, it was stored at 4°C or taken for sectioning.

Sectioning of Tissue

Brains were placed in a small disposable cuvette filled with Richard-Allan Scientific Neg 50™ solution and placed over dry ice as to encase the brain in a solid block of the Richard-Allan Scientific Neg 50™ solution. The frozen block was then removed from the cuvette and placed on the stand in a Leica CM 1850 Cryostat. Brains were sectioned at a range of thicknesses (20 μm-40 μm). The thickness of the slices was determined by the integrity of the tissue, the percentage of the perfusant and the specific planned experiment. Each slice was placed in 1 of 5 wells, sequentially placing a slice in the next well. This way the complete collection of slices in each well provided a representative profile of the brain. Slices designated for the pre-mounted immunohistochemistry protocol were placed in a petri dish for immediate mounting onto a microscope slide (Fisherbrand® Superfrost® Plus Microscope Slides).

Immunohistochemistry

Free-Floating — Brain sections acquired from the cryostat were placed on staining nets to prepare them for washes. The slices were washed 3 times using 0.1 M Tris Buffer (0.1 M TB: 13.22 g Tris-HCL and 1.93 g Trizma base in 1 L of aqueous solution), each wash lasting 5 minutes. They were then washed 3 times with 0.1 M Tris Buffer Saline (0.1M TBS: 8.76 g NaCl in 1 L TB), each wash lasting 5 minutes. During the washes, the incubation solution was made

and cooled prior to incubation. The incubation solution uses TBS as its solvent and consists of 1% NGS and 0.10% Triton-X. The sections were then taken from the staining net and placed in a test tube containing 500 μL of incubation solution. The primary antibody (or primary antibodies) was then added to the incubation test tubes at the desired concentration, and the sections were incubated in the antibody solution at 4°C for 72 hours.

After the primary antibody incubation period, the sections were taken and placed on staining nets for washing. The sections were washed 10 times using 0.1 M Tris Buffer Saline Triton-X (TBST: 1 mL Triton-X in 1 L TBS). Following this wash, the slices were incubated with a secondary antibody bound to an ALEXA flurophore (1/500) in 2 mL of incubation solution for 1 hour at 37°C in the absence of direct light. After the incubation, slices were washed 5 times using 0.1 M TBST, each wash lasting 5 minutes. They were then washed 4 times using with 0.1M TB, each wash lasting 5 minutes.

After the last wash, the slices were mounted onto a microscope slide with a small paintbrush and sealed with Vectashield® mounting medium and Fisherfinest® Premium Cover Glass. These slices were then stored at 4°C in the absence of light.

Pre-mounted Protocol — Brain sections that were separated for mounting during cryostat sectioning, or slices taken from the representative wells were mounted onto microscope slides. These slides were then covered from direct light and allowed to dry for 10 minutes. Once the sections were aptly attached and dried onto the slide, washing began. Although the washes follow the same conditions as the Free-Floating protocol they took place in petri dishes due to the size of the microscope slide. The incubation solution had the same make up as above, but the solution and the slides were incubated in the following manner. After the wash sequence, the slides were left to dry for 10 minutes in the absence of direct light. A thin layer of nail polish was

added to surround the brain sections during incubation, this served to keep the incubation solution from spilling over the sides of the slide. The slides were then placed in a small humidified chamber and 500 µL of primary incubation solution were added on the top of each section to each slide. Trying to not break the surface tension created by the incubation solution, a cover slip was added as to prevent evaporation and to promote the homogeneity of the solution over the brain tissue sections.

After incubation with the primary antibody, the protocol for washing the sections is the same as the free-floating protocol. Prior to incubation with the second antibody, the slides were left to dry for 10 minutes. To incubate the sections with the secondary antibody, 500 µL of secondary incubation solution (1/500) were added to the slides. These were then placed in the humidified chamber on a rotating table at room temperature and incubated for an hour. After secondary antibody incubation, the same washing and sealing procedures as used for the free-floating sections were followed.

Fluorescent Microscopy and Image Acquisition

Slides were examined using a Leica DM 6000B fluorescent microscope. Images were acquired via SimplePCI.

Cell Counting

Cell counts were conducted on the brain slices of one wild type animal. The counts were conducted on images taken from the brain strucutres of interest (cortex and the thalamus) in a

coronal slice where the hippocampus, cortex and thalamus were present. More specifically, 40x magnification images were taken of specific regions within the targeted structures. Target cells were marked on the image display of the SimplePCI software and this marked image was then superimposed on the same sample field but exposed to a different wavelength. This revealed both areas of co-localization as well as cells that did not co-localize. Counts for both of these, as well as reverse counts were conducted when examining the slides. A total of 50 cells were counted for regions of interest within the cortex and thalamus.

Statistical Analysis

Chi-Square tests were conducted to test for an association between brain region and gene expression for the counts taken on the section analyzed. A confidence interval was calculated for the true difference between regional proportion of co-localization between ankyrin-G and *Scn8a* for the counts taken on the section analyzed. Statistical analysis was not done on hippocampal counts because the sample cell count was too small for each individual region.

Results

Optimization of $Na_v1.6$ Antibody

To evaluate the distribution of the expression of *Scn8a* ($Na_v1.6$) in various brain regions an accurate marker for $Na_v1.6$ is needed. We used an anti-*Scn8a* (Millipore Rb Polyclonal Lot: 1986228) antibody to label $Na_v1.6$. We found that brain tissue perfused with 1% PFA resulted in the most specific, restricted to the axonal initial segment of axons where *Scn8a* is expressed, and most robust signal (Figure 1). We also found that to maintain the integrity of the 1% PFA tissue it is best to utilize the pre-mounted protocol in order to help maintain the integrity of the sections. This was not necessary when 4% PFA was used. (Figure 2).

Optimization of Ankyrin-G, Glutamate Decarboxylase (GAD-67) and GABA Antibodies

Prior findings in our laboratory suggested reduced *Scn8a* expression in interneurons lead to the generation of SWDs (Makinson 2014). We first sought to evaluate the distribution of the expression of *SCN8A* in inhibitory cell types. For this we needed antibodies that recognized general inhibitory cell markers. We also needed an antibody that labels the axon initial segments of inhibitory neurons since this is the primary site of *Scn8a* expression (Grub and Barrone 2010). We originally planned on using a primary GABA antibody (Abcam Gpig Polyclonal ab17413 Lot: GR68760-1) which tags gamma-aminobutyric acid; the primary inhibitory neurotransmitter of the mammalian central nervous system. The GABA antibody that we were going to use is known to label the soma and the proximal processes of inhibitory neurons. However, preliminary

testing of this antibody showed that it was not specific for GABA or inhibitory cell types under the conditions that are required to detect *Scn8a* (Figure 3).

We then attempted to use the anti-GAD-67 (Millipore Ms pAb Lot: NG1839533) instead of the anti-GABA antibody to label GABAergic neurons. The anti-GAD-67 primary antibody mainly labels the soma of GABAergic neurons; it binds to glutamate decarboxylase which is involved in the production of GABA. In Figure 4 we can see the successful labeling with GAD-67 in 1% PFA. However, in order to detect co-localization with the *Scn8a* label we were in need of a marker which bridged the somatic labeling of the anti-GAD-67 antibody and the axonal labeling of the anti-*Scn8a* antibody. We decided to use an anti-ankyrin-G antibody (Neuronmab Ms pAb clone N106) which labels all neurons from the start of the axon (somato-axonal boundary) to the end of the axon initial segment (Kaech et al., 2005). We then tested to see if ankyrin-G would also maintain its specificity when used on 1% PFA perfused tissue (Figure 5). Knowing that the conditions of the ankyrin-G, GAD-67 and *Scn8a* antibodies were compatible we attempted to observe GAD-67 and *Scn8a* co-localization. We allowed the fluorescent label to be the same for ankyrin-G and GAD-67 because we did not aim to differentiate between the two, we only aimed to use ankyin-G to mark the axon of the GAD-67 labeled inhibitory neurons. We set up a triple labeled pre-mounted immunohistological reaction (Anti-GAD-67, Anti-Ankyrin-G and Anti-$Na_v1.6$) but due to the high background generated from the use of the three antibodies, analysis of the images acquired was not possible (Figure 10). However, compatibility of the ankyrin-G staining conditions with *Scn8a* staining conditions lead to a dual-label immunohistochemical reaction allowing us to explore the proportion of the general neuronal sample expressing *Scn8a*.

Tomato ROSA Reporter Mice

We then turned to using a mouse line that uses a ROSA reporter gene to endogenously express a red fluorescent protein on the membrane of neurons expressing Cre recombinase. By crossing the ROSA line with a transgenic line that only expresses Cre recombinase in inhibitory GABAergic neurons (DLX-Cre), we were able to generate progeny that only expressed the red fluorescent protein (characteristic of tomato ROSA+ mice) in GABAergic neurons of the brain. In the brain tissue of these animals, the red fluorescent protein was expressed on the plasma membrane of these GABAergic neurons, which allowed for identification of the soma, dendrites, and axon (Figure 6). Therefore, this allowed us to explore the expression of *Scn8a* at the axon initial segment in inhibitory cell types.

Counts of *Dlx*-expressing cells co-localized with *Scn8a*

Table 1 shows the counts of *Dlx*+ cells (cells expressing Dlx) expressing *Scn8a* and the counts of *Scn8a*+ cells (cells expressing *Scn8a*) expressing *Dlx*. In our sampling, we observed that the greatest proportion of *Dlx*+ cells expressing *Scn8a* occurred in cortical layer 2/3 as well as CA1 in the hippocampus, both areas having 37% co-localization. We also observed that the lowest areas of co-localization were cortical layers 4 and 5 as well as the reticular nucleus of the thalamus, each with 16% co-localization. This cell count was generated from images acquired at 40X magnification by the Leica DM 6000B fluorescent microscope using SimplePCI software. TomatoROSA+ Cre *Dlx*+ mice were perfused using 1% PFA, the brains were sectioned at 30 μm and stained with the aforementioned anti-*SCN8A* antibody and a goat anti-Rabbit ALEXA 488 secondary antibody (a flurophore) using the free floating protocol. Figure 9 shows the

immunohistochemical stain and points out the cortical areas of interest where the counts took place. Figure 7 shows the representative co-localization observed when counting the cells.

Scn8a is differentially expressed in *Dlx*+ cells in various cortical layers

Table 2 shows the observed versus expected cell counts of *Scn8a*+ cells in a *Dlx*+ cell sample from one animal. The expected values were generated from the product of the proportion of the total values and the totals of each row (i.e. if the proportion of cells co-localizing in the cortex is 24%, and there is no difference in *Scn8a* expression by cortical layer, then each layer is expected to have 24% co-localization) . A chi-Squared statistical analysis was conducted on these counts. With 4 degrees of freedom and a chi-Square value of 15.6114 a p-value of less than .005 is observed. This allows us to conclude that the expression of *Scn8a* in inhibitory cells varies by region. In other words, *Scn8a* is differentially expressed in *Dlx*+ cells of the cortex.

Counts of ankyrin G+ cells expressing *Scn8a*

Table 3 shows the counts of ankyrin G+ cells expressing *Scn8a* and counts of *Scn8a*+ cells expressing ankyrin-G. In our sampling, we observed that the greatest proportion of ankyrin G+ cells expressing *SCN8A* occurred in cortical layers 1 and 2/3 having 51% and 62% co-localization respectively. We also observed that the lowest areas of co-localization were the reticular nucleus of the thalamus and the VLT with 18% and 19% co-localization, respectively. This cell count was generated from images acquired at 40X magnification by the Leica DM 6000B fluorescent microscope using SImplePCI software. WT were perfused at 1% PFA, the brains were sectioned at 30 μm and stained with anti-*SCN8A*, anti-ankyrin G and their respective secondary antibodies (*SCN8A*: goat anti-rabbit ALEXA 488, Ankyrin-G: goat anti-mouse IgG2α)

using the pre-mounted protocol. Figure 8 shows the immunohistochemical stain and points out the areas of interest where the counts took place. Figure 9 shows the representative co-localization observed when counting the cells.

Scn8a is differentially expressed in ankyrin-G+ cells of the cortex and thalamus

Table 4 shows the observed versus expected cell count of *Scn8a*+ in an ankyrin-G+ cell sample. The expected values were generated from the product of the proportion of the total values and the totals of each row. A Chi-Squared statistical analysis was conducted on these counts. With 4 degrees of freedom and a Chi-Square value of 18.01379 a p-value less than .005 is observed. This allows us to conclude that there is differential expression of *Scn8a* in ankyrin-G+ cells in different cortical layers. In other words, the proportion of ankyrin-G cells expressing *Scn8a* is associated with the cortical layer within which they reside.

Table 5 shows the total counts of ankyrin-G+ cells expressing and not expressing *Scn8a* in the cortex and thalamus. Using these counts a 95% confidence interval for the true difference of population proportions was calculated. Held to an alpha value of 0.05 the interval that resulted was 18 to 34% co-localization. We can interpret this as there being a statistically significant difference between the proportions of ankyrin-G+ cells expressing *Scn8a* in the cortex and the thalamus. In other words, *Scn8a* is differentially expressed in ankyrin-G+ cells depending on whether the neurons are in the cortex or in the thalamus. The sample difference in proportions between the cortex and thalamus also allows us to provide evidence for their being a greater level of co-localization in the cortex when compared to the level of co-expression in the thalamus.

Discussion

Effect of fixative concentration in tissue on anti-$Na_v1.6$ labeling

Using 1% PFA perfused tissue for anti-$Na_v1.6$ immunolabeling gave us the most specific labeling of $Na_v1.6$ which known to be expressed in the axon initial segment of neurons. Attempting to conduct labeling with higher PFA concentrations or any other fixative at a concentration that would crosslink tissue proteins more than the 1% PFA may lead to misleading and inaccurate $Na_v1.6$ labeling. The Millipore polyclonal anti-$Na_v1.6$ antibody that we used targets the intracellular loop between the II and II domain of $Na_v1.6$. This may suggest that the antibody's access to its epitope may be a determinant of the accuracy of the immunohistochemical labeling. The access of the antibody to this intracellular domain may be affected by the concentration of the fixative used to perfuse the tissue. Perfusing tissue with a fixative results in the cross linking of various proteins that constitute the tissue. It would then make sense that an increase in the concentration of the fixative would result in more widespread and denser cross-linking of tissue proteins. If membrane components and proteins are fixed more densely, the access that the anti-$Na_v1.6$ antibody has to its epitope will certainly be diminished. This may not only result in the lack of accurate labeling but may generate non-specific labeling as is shown by the somatic labeling by the anti-$Na_v1.6$ antibody that occurs when using 4% PFA (Figure 1).

It would then follow that the results gained from such experiments where the tissue is perfused with 4% PFA should take into consideration the possibility of non-specific labeling. This is especially important for experiments that evaluate fluorescent intensity as a result of $Na_v1.6$ immunolabeling such as Wart et al.(2007) and Xie et al. (2013). Many of the

commercially available antibodies recognize this same intracellular loop. It follows then that regardless of the tissue under study, may it be retinal tissue, dorsal root ganglia, or any other tissue, the fixative used will affect the specificity of the labeling. If the specificity and accuracy of the antibody is affected, the optical data (i.e. fluoresecent intensity) gathered will also be affected. It may be argued that what is important is not the absolute intensity but the relative intensity; however one must also consider that optic data may be incorrectly representing the distribution of $Na_v1.6$ expression. Based on my data, use of 1% PFA fixative or a fixative concentration resulting in the same level of cross linking as 1% PFA would be predicted to result in specific and reliable labeling of $Na_v1.6$ in cerebral tissue.

Looking at isotype in the triple label reaction: GAD-67, ankyrin-G and $Na_v1.6$ stain

In planning the triple stain immunohistochemical reaction to observe *SCN8A* expression in inhibitory cells we had to consider the isotype and animal host of each of the antibodies. It is these two characteristics of an antibody that allow for fluorescent characterization, thus it is essential to consider these prior to attempting an immuhistochemical reaction. The anti-ankyrin-G antibody and the anti-GAD-67 antibody both shared the mouse as their host. When this occurs, researchers will usually verify that the isotype of these "same host antibodies" vary. For our experiment, we decided otherwise.

Both antibodies have the same IgG2α isotype but we decided that there was a possibility that it would work to our advantage. As stated earlier, the fluorescent tag attached to the primary antibody depends on the isotype of the antibody. Usually two antibodies having the same fluorescent tag causes confusion, and gives undesired results. Yet, the function of the ankyrin-G label, as initially determined, was to provide a link between the GAD-67 labeling and the *Scn8a*

labeling in order to confirm that the same neuron was being examined. In this way, allowing the GAD-67 fluorescent label to be the same as the ankyrin-G fluorescent label would still allow us to observe the co-localization of *Scn8A* and GAD-67. The ankyrin-G stains (Figures 7 and 11) proved to be relatively low in background and highly specific. The GAD-67 stains (Figure 4) also show relatively low background. It followed then that using them in tandem would not result in an excessively high background signal. However, what we found was that the background signal was too high and rendered the images of the triple stain un-interpretable (Figure 10). This suggested the need of a unique fluorescent tag for each individual primary antibody regardless of the purpose of the label in generating optically analyzable images.

Using endogenously expressed fluorescent protein as a marker for cell type

In our experiments we sought to examine the expression of *Scn8a* in inhibitory cells. To do so we needed a marker that tags inhibitory neurons and allows for co-localization with the axonally restricted $Na_v1.6$. As described above, our triple antibody immunohistochemical reaction unfortunately resulted in too high of a background to analyze. To overcome this problem, we decided to endogenously label inhibitory cells through the implementation of a tomato ROSA reporter gene. Using the ROSA reporter we can attain whole neuronal expression of a fluorescently labeled protein bound to the membrane of the neuron. If a mouse line has the correct genotype (i.e. expressing Cre only in GABAergic neurons) then accurate labeling of GABAergic neurons with much less background than antibody labeling is possible. Using this tissue allows for single antibody immunohistochemical reactions to result in a dual label image. Similarly, if a double antibody immunohistochemical reaction were to be conducted it would result in a triple label image.

Implications of differential expression of *Scn8a*

It is known that absence seizure generation results from a disruption in the thalamocortical circuitry responsible for normal oscillatory patterns found during sleep (McCormick & Bal, 1997). To propose a model for the generation of absence seizures, I propose the following thalamocortical circuit is involved: Layer 6 of the cortex serves as a waypoint between intercortical and subcortical connections in the brain. The pyramidal neurons of layer 6 synapse on the GABAergic neurons of the reticular nucleus of the thalamus as well as neurons of cortical layer 4 (Zhang and Deschenes 1998; Mercer et al., 2005). Layer 6 pyramidal neurons receive their inputs from both the thalamocortical projection neurons and the pyramidal cells of layer 5. Layer 5 pyramidal neurons receive their input in part from connections associated with neurons in layer 2/3 (Mercer et al., 2005). And finally layer 2/3 receives input from the pyramidal cells present in layer 4 (Yoshimura et al., 2005).

We found that the differences in proportion of co-localization between anti-Na_v 1.6 and GAD-67 amongst the cortical layers are significant. In other words, there is an association between the cortical layer and the proportion of $Na_v1.6$ expression in a *Dlx+* population. We also found that by using the ankyrin-G stain and looking at co-localization of *Scn8a* and ankyrin-G in different brain regions we could survey *Scn8a* expression in the representative neuronal population. It is also interesting to observe that the reverse count, that of cells expressing *Scn8a* also expressing ankyrin-G, shows that *Scn8a* may be expressed in non-neuronal cell types to some extent. Ankyrin-G labels the axon initial segment for both inhibitory and excitatory neurons. Knowing this, cell counts acquired at the various regions should reflect the amount of neurons within that sample within that region. In other words, we can assume that the calculated

proportion of co-localization is the proportion of neurons — excitatory and inhibitory — expressing *Scn8a*.We found that *Scn8a* is differentially expressed in the cortical layers as well other brain regions.

Our findings may provide the basis for an explanation of why *Scn8a* mutations often result in absence epilepsy and SWD generation. The up-regulation of *Scn8a* and *Scn1a* observed in the cortical layer of a congenic absence epilepsy model that does not involve a sodium channel mutation illustrates the importance of *Scn8a* in the development of absence epilepsy (Klein et al., 2003) In addition, decreased expression of *Scn8a* in GABAergic neurons also results in SWD generation, implying the importance of *Scn8a* expression in GABAergic neurons to SWD generation (Makinson 2013). We observed that the highest proportion of GABAergic neurons expressing *Scn8a* occurs in cortical layer 2/3 and that the lowest proportion of GABAergic neurons expressing *Scn8a* was in the thalamus. I propose that the involvement of a mutated *Scn8a* gene in absence seizure generation results from the effect the mutation has on *Scn8a* expression of neurons in the cortical layer 2/3. In mice with reduced expression of *Scn8a*, the excitability of both GABAergic neurons and excitatory neurons in layer 2/3 would theoretically be affected; *Scn8a* expression in both of these cell types and differential expression in this layer has been verified by our results and the results of Klein et. al. (2003). Our results show that only a smaller proportion of the neurons in the thalamus as opposed to the cortex express *Scn8a*. Our results also show that a smaller proportion of GABAergic neurons express *Scn8a* in the reticular nucleus of the thalamus as compared to the cortex and the hippocampus. In mice with reduced *Scn8a* expression, the excitability of neurons expressing *Scn8a* is affected. Effectively, if there is a lower proportion of neurons that express *Scn8a* within a region then that region may theoretically be less affected by an *Scn8a* mutation. Conversely, if there is a higher proportion of

Scn8a positive cells within a certain region, then that region might be affected by the mutation more potently. Drawing a parallel to this logic, layers 2/3 have high *Scn8a* expression both in the total neuronal population and in the GABAergic neuronal population. The thalamus on the other hand has fewer *Scn8a* positive cells in the total and in the GABAergic neuronal population.

I propose that the signaling activity of the cortex is affected by *Scn8a* mutations in the following way. First, a proportion of inhibitory neurons in cortical layer 2/3 will have dampened signaling and thus result in less inhibition in this cortical layer. This reduction in signaling will result in a decrease in inhibition for the pyramidal neurons of layer 2/3 projecting to layer 5 as well as a decrease in inhibition for the pyramidal neurons of layer 5 who receive input from cortical layer 2/3. In other words, the loss of inhibition not only affects neurons within layer 2/3 but also those in layer 5. This loss of inhibition may be responsible for the maintenance of a positive feedback loop that results from layer 6 collateral excitation of layer 4 followed by excitation of layer 2/3 followed by excitation of layer 5 followed by re-excitation of layer 6 and so forth.

Second, the reduction in inhibition in layer 2/3 makes it more prone to neuronal hyper-excitation from active thalamocortical neurons that project to it (Viaene et al., 2011). Cortical layer 2/3 is also known to have vast reaching intracortical connections (Thomsom and Bannister 2003). The ample network of excitatory neurons that synapse in layer 2/3 may enter a high-synchronous firing state if necessary inhibition provided by *Scn8a* expressing interneurons is absent.

The generation of this hyper-active and hyper-synchronous signal by thalamocortical neurons projecting to layer 2/3 of the cortex may result in the pre-SWD signal observed by

Seidenbecher et al., 1998. The engagement of the intracortical loop by the thalamocortical neurons would engage the thalamocortical circuitry in a short-lived cyclical synchronous state with the cortex, like the one observed in absence seizures. Unlike generalized tonic-clonic seizures observed in *Scn1a* mutants that result from a whole brain reduction of inhibition, the model I propose not only shows a cortical positive feedback loop and the development of thalamocortical synchronicity but also shows that the GABAergic neurons of the reticular nucleus of the thalamus will increase their inhibition over thalamocortical neurons as a cause of corticothalmic projections from layer 6. The inhibition that the GABAergic neurons of the reticular nucleus provide to the thalamus could explain why SWDs are short-lived. The bursting nature of certain thalamic cells could also explain why SWDs are spontaneous. I say this because ethosuximide, the drug to treat absence epilepsy, is thought to affect T-type Ca^{2+} voltage-gated channels. These very channels are involved in the rhythmic bursting nature of thalamic neurons (Gomora et al.,2001). It would make sense then that if the bursting of these neurons is reduced by blocking T-type Ca^{2+} voltage-gated channels then the hyperactive circuit would be prevented and the frequency of SWDs would decrease, as is observed in Papale et al., 2009. Although this is one possible of the source of thalamocortical excitation, intrathalamic interactions may also be involved. Figure 11 gives a schematic to the proposed model.

Conclusion and Future Directions

In conclusion, I propose that the mechanism for absence seizure generation in *Scn8a* mutant mice may be dependent on the reduced expression of *Scn8a* in layer 2/3 of the cortex. In this study I evaluated the expression of *Scn8a* in different brain regions and cell types. The evaluation of *Scn8a* in excitatory cell types should also be studied to provide further evidence for or against the proposed mechanism. We should also explore *Scn8a* expression in various GABAergic neurons populations as well as various excitatory neuronal populations to further elucidate the mechanisms by which absence seizures are generated.

We have shown that reducing *Scn8a* expression in the GABAergic neurons population causes SWDs (Makinson 2014). It would be interesting to see if the reduction of *Scn8a* expression in GABAergic neurons localized in the reticular nucleus of the thalamus, or localized in the cortex, would also result in the characteristic SWDs of absence seizures.

The mechanism of absence seizure generation merits further exploration not only because of the potential clinical benefit relating to its understanding, but it would also shed light on understanding neuronal communication as a whole as well as the function of sodium channels in the brain.

Figures and Tables

Table 1. Cell counts of *Dlc*+ neurons expressing *Scn8a* and counts of *Scn8a*+ neurons expressing *Dlx*.

	Co-localization of *Dlx* and *Scn8a* in various brain regions					
Brain Region	Proportion of *DLX*+ Cells Expressing *SCN8A*			Proportion of *Scn8a*+ Cells Expressing *Dlx*		
	No. of *Dlx*+ Cells	No. of *Scn8a*+ Cells	Co-localization (%)	No. of *Scn8a*+ Cells	No. of *Dlx*+ Cells	Co-localization (%)
Cortex						
Layer 1	44	9	21	42	4	10
Layer 2/3	108	40	37	126	16	13
Layer 4	63	10	16	127	12	10
Layer 5	56	9	16	179	8	5
Layer 6	77	16	20	172	7	6
Total	348	84	24	646	47	7
Thalamus						
nRT	50	8	16	127	30	24
VLT	0	0	0	24	0	0
Hippocampus						
CA1	19	7	37	84	3	4
CA2	19	5	21	51	4	8
CA3	23	6	26	52	2	4
DG	22	8	36	59	4	7
Total	83	25	30	246	13	5

Table 2. Observed counts vs expected counts of *Dlx*+ cells expressing *Scn8a*.

	Expression of *Scn8a* in *Dlx*+ Cells				
	Yes		No		
Cortical Layer	Observed	Expected	Observed	Expected	Total
Layer 1	9	11	35	33	44
Layer 2/3	40	26	68	82	108
Layer 4	10	15	53	48	63
Layer 5	9	14	47	42	56
Layer 6	16	19	61	58	77
Total	84		264		348

.001<p-value<.005 Chi-Square=15.6114 df=4

Table 3. Cell counts of ankyrin-G+ neurons expressing *Scn8a* and counts of *Scn8a*+ neurons expressing ankyrin-G.

	Co-localization of AnkyrinG and *Scn8a* in various brain regions					
	Proportion of Ankyrin G+ Cells Expressing *Scn8a*			Proportion of *Scn8a*+ Cells Expressing Ankyrin G		
Brain Region	No. of Ankyrin-G+ Cells	No. of *Scn8a*+ Cells	Co-localization (%)	No. of *Scn8a*+ Cells	No. of Ankyrin-G+ Cells	Co-localization (%)
Cortex						
Layer 1	49	25	51	30	29	97
Layer 2/3	89	55	62	69	40	57
Layer 4	115	36	31	66	46	70
Layer 5	114	46	40	142	97	68
Layer 6	110	50	46	114	92	81
Total	477	212	44	421	304	72
Thalamus						
nRT	57	10	18	53	22	42
VLT	63	12	19	18	9	50
Total	120	22	18	71	31	44

Table 4. Observed versus expected counts of ankyrin-G+ cells expressing *Scn8a*.

	Expression of *Scn8a* in Ankyrin G+ Cells				
	Yes		No		
Cortical Layer	Observed	Expected	Observed	Expected	Total
Layer 1	25	22	24	27	49
Layer 2/3	55	40	34	49	89
Layer 4	36	51	79	64	115
Layer 5	46	51	68	63	114
Layer 6	50	49	60	61	110
Total	212		265		477

.001<p-value<.005 Chi-Square=18.01379 df=4

Table 5. Shows the confidence interval for the difference of proportions in co-localization.

	Expression of *Scn8a* in ankyrin G+ Cells		
Brain Region	Yes	No	Total
Cortex	212	265	477
Thalamus	22	98	120
Total	234	363	597

alpha=.05 95% CI= (17.8,34.2)

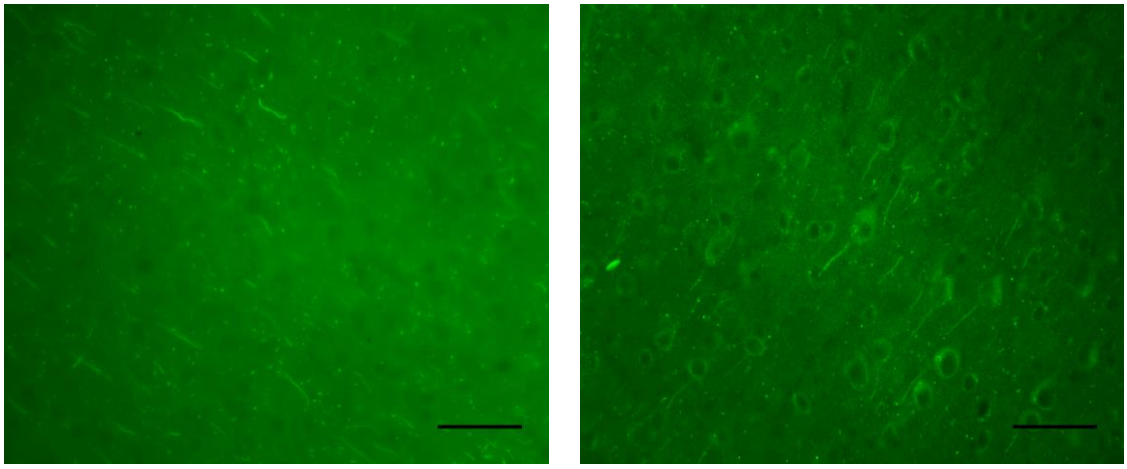

Figure 1.Anti-$Na_v1.6$ staining in 1% PFA vs 4% PFA. A. Free floating 1% perfused tissue B. 4% perfused tissue. Note the main differences in immunohistochemical tagging: the cell bodies are tagged in the 4% tissue but not in the 1% tissue. We can conclude that unspecific labeling occurs when using the anti-$Na_v1.6$ antibody with 4% perfused tissue, it is therefore best to conduct experiments with 1% perfused tissue. (Scale bars 50 μm)

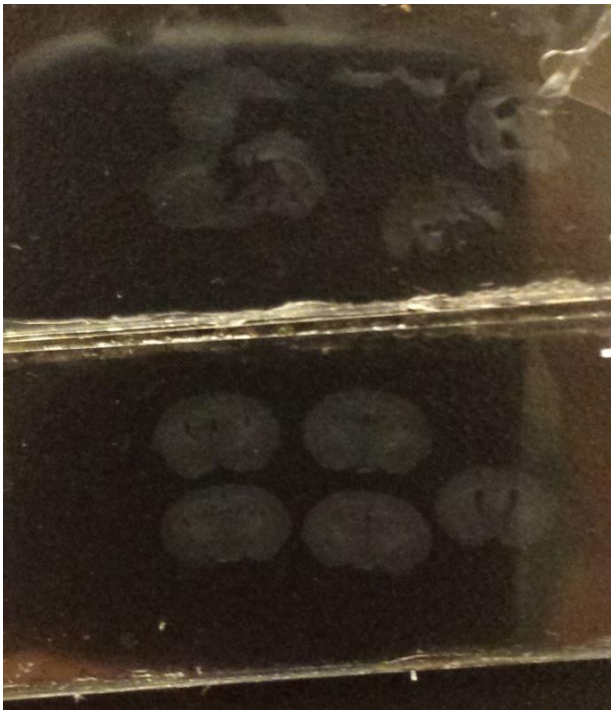

Figure 2. General integrity of 1% and 4% PFA tissue. The bottom slide is 4% PFA perfused tissue mounted after the immunohistochemistry protocol. The top slide is 1% perfused PFA tissue also mounted after the immunohistochemistry protocol. Note how the 4% PFA is more intact than the slightly warped and less intact 1% PFA perfused tissue. To look at gene expression by region it is necessary to keep the brain section as intact as possible. Conducting the pre-mounted protocol with 1% PFA results in similar tissue preservation as 4% PFA.

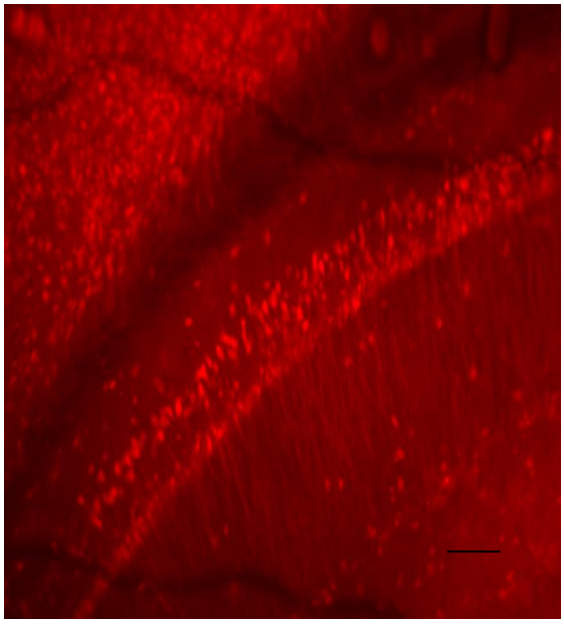

Figure 3. pAb GABA failed stain in hippocampal section. In this image we can see how our abcam GABA antibody lost specificity and no longer serves as a tag for GABAergic neurons under the 1% PFA conditions. In this hippocampal slice taken at 10x we can see how even pyramidal neurons are stained with the inhibitory marker.(Scale bars show a 100 μm).

Figure 4. Anti-GAD-67 stain of the nRT in 1% PFA tissue. In this image we can see the GABAergic neurons characteristic of the nRT labeled by the anti-GAD-67 antibody. The reticular nucleus is the area in the white oval to the right of the oval we can see the lack of GABAergic neurons in the thalamus. It is also important to note the labeling is mostly somatic, this led to the need for a somato-axonal bridge between GAD-67 labeling and $Na_V1.6$ labeling. (Scale bar 100 μm)

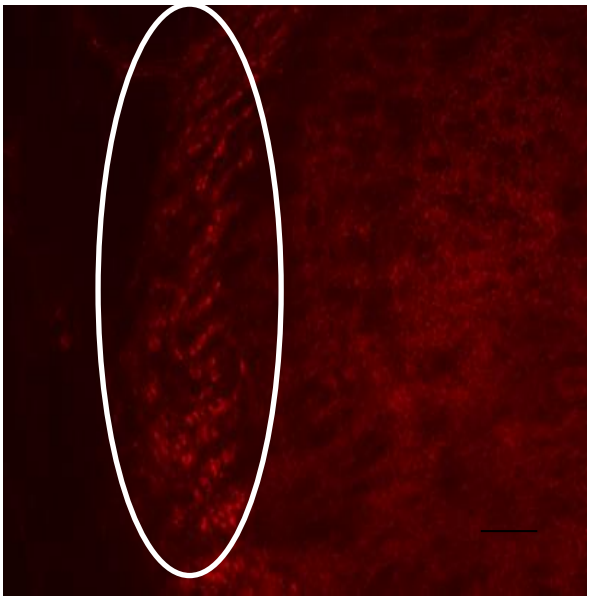

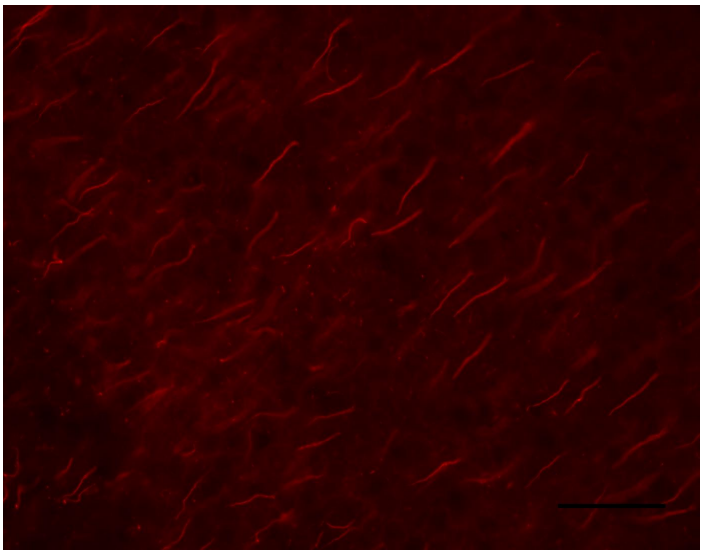

Figure 5. Anti-ankyrin-G immunolabeling of 1% PFA tissue. This image shows the immunolabeling of ankyrin-G in the cortex. Note that the stain is specific to the initial segment of neurons. (Scale bars 50 µm).

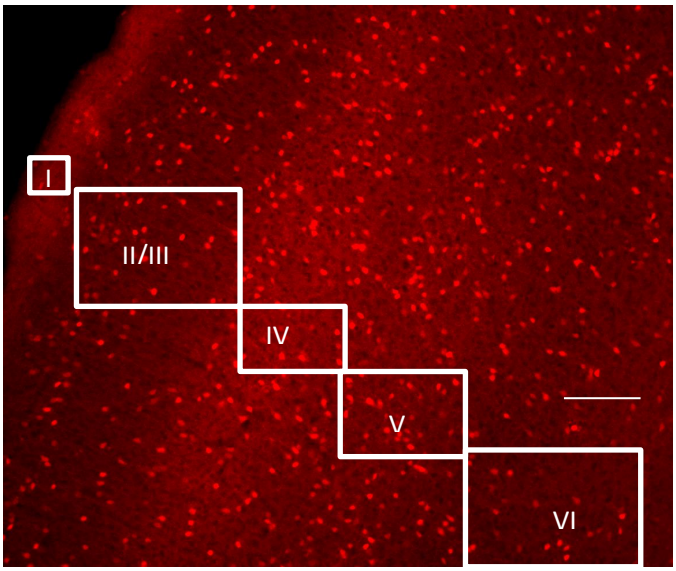

Figure 6. Image of endogenously fluorescent DLX+ cells. In this image, taken at 10x, we can observe the endogenously expressed red fluorescent protein. We can also note the various cortical layers which were the regions of interests for our counts. The Roman numeral inside the box represents the cortical. (Scale bar is 50 µm).

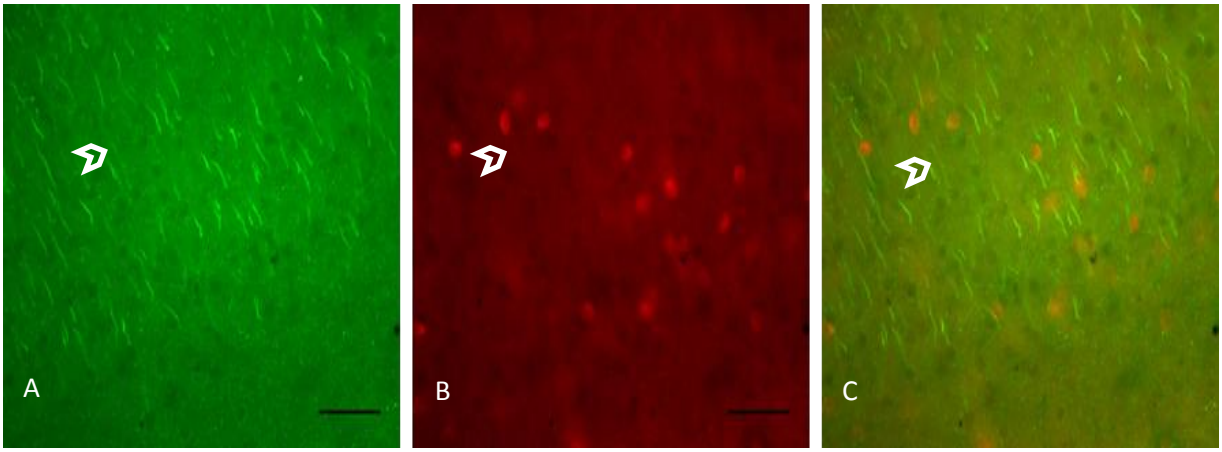

Figure 7. Characteristic co-localization of *Scn8a* and *Dlx*. A. Anti-$Na_v1.6$ B. Endogenous *DLX*+ red fluorescent tagging C. Overlay of the two different filters. The white arrow in each pane shows a representative area of co-localization between *Scn8A* and *Dlx*. (Scale bars 50 μm)

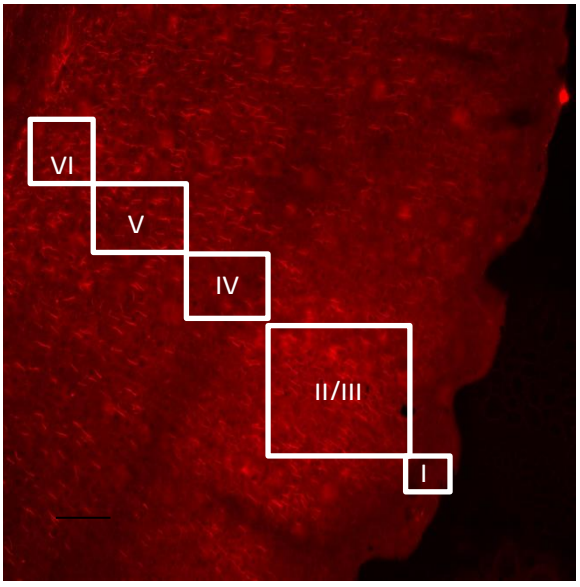

Figure 8. Anti-ankyrin-G staining of the cortex. This image shows anti-ankyrin-G staining in the cortex. Roman numerals correspond to the cortical layer.

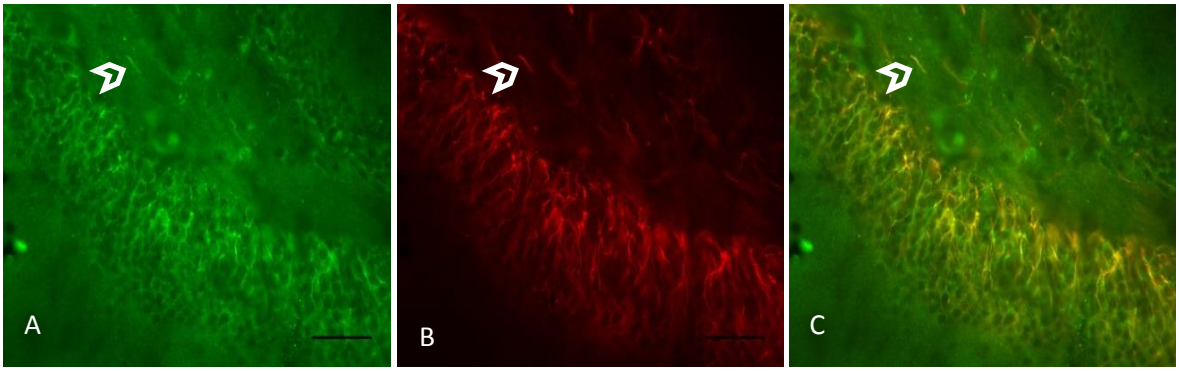

Figure 9. Co-localization between ankyrin-G and *Scn8a in hippocampal slice*. A. Anti-*Scn8a* stain B. Anti-ankyrin G stain. C. Overlay between the two filters. The white arrow in each pane shows a representative area of co-localization between *Scn8a* and ankyrin-G. (Scale bars 50 μm)

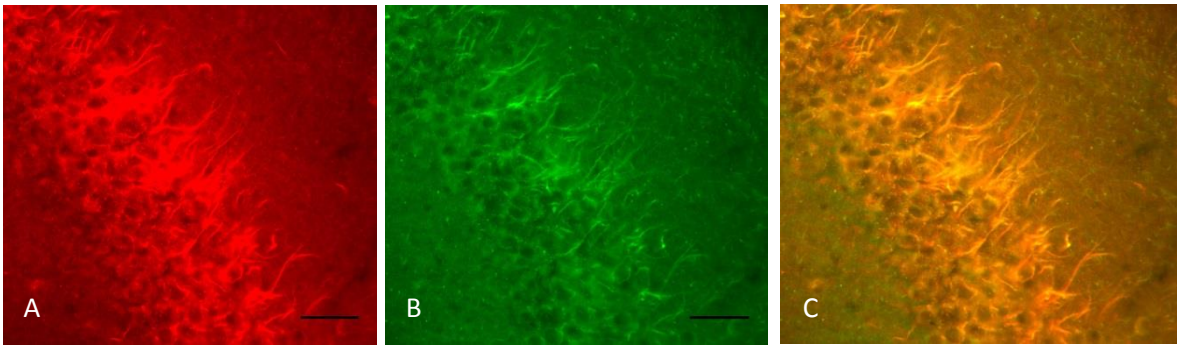

Figure 10. Failed triple stain. A. Shows the fluorescent label of ankyrin-G and GAD 67 combined. B. Shows the fluorescent label of *Scn8a*. C. Shows both filters. Here we can see that the background generated by the fluorescent label for ankyrin-G and GAD67 produces images where counts cannot be made.

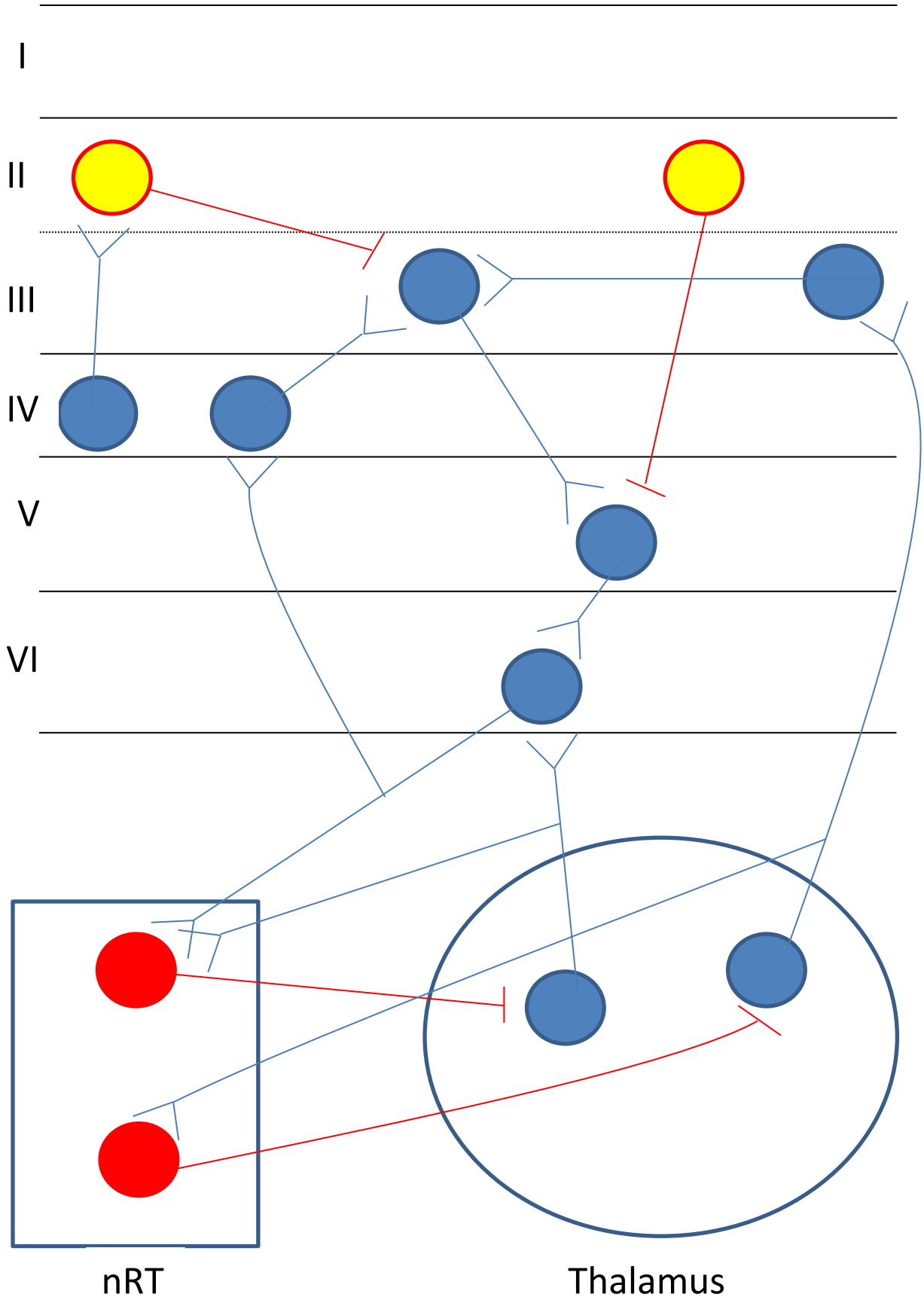
I
II
III
IV
V
VI
nRT
Thalamus

Figure 11. Model circuitry for absence seizure generation. In this schematic the box on the left represents the reticular nucleus of the thalamus. The ellipse on the right represents the thalamus. Each section labeled with a Roman numeral represents that cortical layer. Blue circles represent excitatory neurons while red/yellow ones represent inhibitory neurons. The synapses are represented by red lines (inhibitory signal) or blue "forked" lines (excitatory signal). The yellow circles are the inhibitory neurons affected by the Scn8a mutation. Their lack of inhibitory signaling will reduce the inhibition in layers 2/3 and 5. Thalamocortical stimulation of either layer 6 or layer 2/3 can lead to the highly active and synchronous circuitry characteristic of seizures.

References

Buchner, D. a, Seburn, K. L., Frankel, W. N., & Meisler, M. H. (2004). Three ENU-induced neurological mutations in the pore loop of sodium channel *SCN8A* (Na(v)1.6) and a genetically linked retinal mutation, rd13. Mammalian genome : official journal of the International Mammalian Genome Society, 15(5), 344–51. doi:10.1007/s00335-004-2332-1

Cummins, T.R., Dib-Hajj, S.D., Herzog, R.I. and Waxman, S.G. (2005) Nav1.6 channels generate resurgent sodium currents in spinal sensory neurons. FEBS Lett., 579, 2166–2170.

Do, M.T. and Bean, B.P. (2004) Sodium currents in subthalamic nucleus neurons from Nav1.6-null mice. J. Neurophysiol., 92, 726–733.8.

Gomora, J. C., Daud, a N., Weiergräber, M., & Perez-Reyes, E. (2001). Block of cloned human T-type calcium channels by succinimide antiepileptic drugs. Molecular Pharmacology, 60(5), 1121–32. Retrieved from http://www.ncbi.nlm.nih.gov/pubmed/11641441

Grubb, M. S., & Burrone, J. (2010). Activity-dependent relocation of the axon initial segment fine-tunes neuronal excitability. Nature, 465(7301), 1070–4. doi:10.1038/nature09160

Hawkins, N. a, Martin, M. S., Frankel, W. N., Kearney, J. a, & Escayg, A. (2011). Neuronal voltage-gated ion channels are genetic modifiers of generalized epilepsy with febrile seizures plus. Neurobiology of disease, 41(3), 655–60. doi:10.1016/j.nbd.2010.11.016

Isom, L.L., De Jongh, K.S., and Catterall, W.A. 1994. Auxiliary subunits of voltage-gated ion channels. Neuron. 12:1183–1194

Klein, J. P., Khera, D. S., Nersesyan, H., Kimchi, E. Y., Waxman, S. G., & Blumenfeld, H. (2004). Dysregulation of sodium channel expression in cortical neurons in a rodent model of absence epilepsy. Brain Research, 1000(1-2), 102–9. doi:10.1016/j.brainres.2003.11.051

Kaech, S., & Banker, G. (2006). Culturing hippocampal neurons. *Nature Protocols*, *1*(5), 2406–15. doi:10.1038/nprot.2006.356

Lacey, C. J., Bryant, A., Brill, J., & Huguenard, J. R. (2012). Enhanced NMDA receptor-dependent thalamic excitation and network oscillations in stargazer mice. *The Journal of neuroscience : the official journal of the Society for Neuroscience*, *32*(32), 11067–81. doi:10.1523/JNEUROSCI.5604-11.2012

Lefort, S., Tomm, C., Floyd Sarria, J.-C., & Petersen, C. C. H. (2009). The excitatory neuronal network of the C2 barrel column in mouse primary somatosensory cortex. Neuron, 61(2), 301–16. doi:10.1016/j.neuron.2008.12.020

Levin, S.I., Khaliq, Z.M., Aman, T.K., Grieco, T.M., Kearney, J.A., Raman, I.M. and Meisler, M.H. (2006) Impaired motor function in mice with cell-specific knockout of sodium channel *SCN8A* (Nav1.6) in cerebellar purkinje neurons and granule cells. J. Neurophysiol., 96, 785–793

Makinson, C. (2013) Doctorate Thesis Defense (access to this document has been restricted until 2020)

Martin, M. S., Tang, B., Papale, L. a, Yu, F. H., Catterall, W. a, & Escayg, A. (2007). The voltage-gated sodium channel *SCN8A* is a genetic modifier of severe myoclonic epilepsy of infancy. *Human molecular genetics*, *16*(23), 2892–9. doi:10.1093/hmg/ddm248

Maurice, N., Tkatch, T., Meisler, M., Sprunger, L.K., and Surmeier, D.J. (2001). D1/D5 dopamine receptor activation differentially modulates rap- idly inactivating and persistent sodium currents in prefrontal cortex pyramidal neurons. J. Neurosci. 21:2268–2277

McCormick, D.A. and Bal, T. (1997) Sleep and arousal: thalamocortical mechanisms. *Annu. Rev. Neurosci*, ***20,*** *185-215.*

Mercer, A., West, D. C., Morris, O. T., Kirchhecker, S., Kerkhoff, J. E., & Thomson, A. M. (2005). Excitatory connections made by presynaptic cortico-cortical pyramidal cells in layer 6 of the neocortex. Cerebral Cortex (New York, N.Y. : 1991), 15(10), 1485–96. doi:10.1093/cercor/bhi027

Meisler, M. H., & Kearney, J. A. (2005). Review series: Sodium channel mutations in epilepsy and other neurological disorders, *115*(8). doi:10.1172/JCI25466.2010

Meisler, M. H., O'Brien, J. E., & Sharkey, L. M. (2010). Sodium channel gene family: epilepsy mutations, gene interactions and modifier effects. *The Journal of physiology*, *588*(Pt 11), 1841–8. doi:10.1113/jphysiol.2010.188482

National Center for Chronic Disease Prevention and Health Promotion (2011). Targeting epilepsy Improving the lives of people with one of the nation's most Common neurological Conditions. *System*. Retrieved from http://www.cdc.gov/chronicdisease/resources/publications/aag/pdf/2011/Epilepsy_AAG_2011_508.pdf

Papale, L. a, Beyer, B., Jones, J. M., Sharkey, L. M., Tufik, S., Epstein, M., … Escayg, A. (2009). Heterozygous mutations of the voltage-gated sodium channel *SCN8A* are associated with spike-wave discharges and absence epilepsy in mice. *Human molecular genetics*, *18*(9), 1633–41. doi:10.1093/hmg/ddp081

Seidenbecher, T., Staak, R., & Pape, H. C. (1998). Relations between cortical and thalamic cellular activities during absence seizures in rats. *The European journal of neuroscience*, *10*(3), 1103–12. Retrieved from http://www.ncbi.nlm.nih.gov/pubmed/9753178

Steriade M, McCormick DA, Sejnowski (1993) Thalamocortical oscillations in sleeping and aroused brain. Science 262:679-685

Thomson, A. M., & Bannister, a P. (2003). Interlaminar connections in the neocortex. Cerebral Cortex (New York, N.Y. : 1991), 13(1), 5–14. Retrieved from http://www.ncbi.nlm.nih.gov/pubmed/12466210

Van Wart, A. and Matthews, G. (2006) Impaired firing and cell-specific compensation in neurons lacking Nav1.6 sodium channels. J. Neurosci., 26, 7172–7180

Viaene, A. N., Petrof, I., & Sherman, S. M. (2011). Synaptic properties of thalamic input to layers 2/3 and 4 of primary somatosensory and auditory cortices. Journal of Neurophysiology, 105(1), 279–92. doi:10.1152/jn.00747.2010

Wart, A. V. A. N., Trimmer, J. S., & Matthews, G. (2007). Polarized Distribution of Ion Channels within Microdomains of the Axon, 352(August 2006), 339–352. doi:10.1002/cne

Xie, W., Strong, J. a, Ye, L., Mao, J.-X., & Zhang, J.-M. (2013). Knockdown of sodium channel NaV1.6 blocks mechanical pain and abnormal bursting activity of afferent neurons in inflamed sensory ganglia. Pain, 154(8), 1170–80. doi:10.1016/j.pain.2013.02.027

Yoshimura, Y., Dantzker, J.L., Callway, E.M. (2005) Exciatory cortical neurons form fine-scale functional networks. Nature Vol 433. 24 February 2005.

Yu, F.H., et al. 2003. Sodium channel β4, a new disulfide-linked auxiliary subunit with similarity to β2. J. Neurosci. 23:7577–7585.

Zhang, Z. W., & Deschênes, M. (1997). Intracortical axonal projections of lamina VI cells of the primary somatosensory cortex in the rat: a single-cell labeling study. The Journal of Neuroscience : The Official Journal of the Society for Neuroscience, 17(16), 6365–79. Retrieved from http://www.ncbi.nlm.nih.gov/pubmed/9236245